Published in Analytica Chimica Acta 1035 (2018) 32-43

Comparison of different speciation techniques to measure Zn availability in hydroponic media

Encarna Companys[a], Josep Galceran[a,*], Jaume Puy[a], Maria Sedó[a], Ruben Vera[b], Enriqueta Anticó[b] and Clàudia Fontàs[b]

[a]*Departament de Química. Universitat de Lleida and AGROTECNIO, Rovira Roure 191, 25198 Lleida, Spain*

[b]*Departament de Química, Universitat de Girona, 17071 Girona, Spain*

** Corresponding author galceran@quimica.udl.cat*

Abstract

Four analytical techniques are compared: AGNES (Absence of Gradients and Nernstian Equilibrium Stripping), LASV (Anodic Stripping Voltammetry with Linear stripping), DGT (Diffusive Gradients in Thin films) and PIM (Polymer Inclusion Membranes). These techniques have been designed to provide the free ion concentration or a labile fraction, complementarily contributing to an integrated description of speciation and availability. Their simultaneous application to the determination of free Zn concentrations or labile fluxes in seven solutions of a hydroponic medium reveals characteristics of each technique and correlations between their results. All dynamic results can be interpreted in terms of a general theoretical framework on fluxes. Indeed, in techniques under diffusion-limited conditions in the sample, the flux can be split into the free contribution (linearly proportional to the free fraction), plus the contribution of the complexes (where mobility, lability and abundance of complexation are intertwined). A methodology to compute lability degrees is developed. Measurements with PIM devices confirm that

diffusion in the sample solution is not rate limiting, so its flux is proportional to the free metal in the donor solution. A proportionality between the responses of any given two techniques is observed, which suggests that, for the low ligand-to-metal concentration ratios used in the present work, any of these techniques would correlate similarly with uptake, toxic or nutritional measurements.

Keywords: Diffusive Gradients in Thin Films; Absence of Gradients and Nernstian Equilibrium Stripping; Polymer Inclusion Membrane; Voltammetry; Zinc ; Speciation

1. Introduction

Hegemonic paradigms, such as the Free Ion Activity Model (FIAM) [1] and the Biotic Ligand Model (BLM) [2], correlate the toxicity (or nutritional capacity) of a trace metal to the free metal ion concentration (or activity) in the medium in contact with the organism. However, some exceptions to this key role of the free metal ion have been pointed out [3, 4]. The uptake of Zn and Cu by spinach and tomato plants, for fixed free metal ion concentrations ($[Zn^{2+}]$ and $[Cu^{2+}]$), increased when more metal was also bound to ligands [5], indicating that metal complexes might contribute to the uptake by dissociating close to the root surface according to their lability [6]. More recent reports [7-9] also indicate the contribution of complexes, either by their dissociation or by their direct internalization on the roots, in some cases, while the key role of the free metal ion is confirmed in most cases.

So, there is a current debate on the extent of the contribution of the different chemical species towards the resulting uptake of a metal. Clearly, there is a need for knowing not only the equilibrium concentrations (i.e. the distribution of the element amongst different chemical species, which is called the equilibrium speciation of the element), but also the rate of contribution to the uptake from the dissociation of the complexes (i.e. the dynamic speciation) in the medium [10-12]. The answer to this need is the development of analytical techniques able to quantify concrete fractions of an element, such as the concentration of the free fraction or the so-called “labile fraction”. Some of these fractions have shown good correlation with the metals accumulated in plants [13-15]. Central to this development is the improvement of their interpretation, i.e. the assessment of which species and to which extent do they contribute to the fluxes. Comprehensive reviews of the main developments of dynamic and equilibrium techniques have been recently published [12, 16-19].

Free metal ion concentrations can be directly measured by a few techniques. The use of an Ion Selective Electrode (ISE) [20] would be a simple way to determine the free Zn^{2+} concentration, but, up to date, there is no commercial ISE for Zn. Membrane based techniques have also been developed for the determination of the free metal concentration. The Donnan Membrane Technique (DMT) [21] uses a cation exchange membrane to measure free ion concentrations based on Donnan membrane equilibrium. In the Resin Titration Technique[16] and in the Ion-Exchange Technique [22] the analyte is accumulated in an ionic exchange resin. The electroanalytical technique AGNES [19, 23] has proved successful in measuring the free concentration of Zn in a range of systems including natural waters [24-27], dispersions of nanoparticles [28, 29] or wine[30].

Labile fractions are accessed via the dynamic techniques. The general recorded signal of these techniques is an arriving flux of metal to a sensor. Apart from the direct supply of the free metal to this flux, there might be other contributions. In some cases, the complexes might contribute directly (e.g. second wave in stripping techniques [31]), but usually some prior dissociation of the complexes generating free metal is required [32]. The rate of such dissociation (in comparison with the diffusion rate) determines the so-called "lability degree"(ξ) of the complex [33, 34].

One of the classical dynamic techniques is Anodic Stripping Voltammetry (ASV), with many variants such as the one with the application of a linear potential scan in the stripping stage (LASV). Along the deposition stage of any ASV variant, the arriving metal species is reduced to M^0 forming a metal amalgam at the mercury electrode, which is later on stripped from the mercury by oxidation, yielding an intensity current which is the response signal [16]. The correct interpretation of such a signal remains still a challenge, given complications such as the electrodic adsorption of humic matter. Since time ago [35, 36] operational correlations of ASV lability and bioavailabity were indicated. More recent investigations have also correlated stripping signals with the uptake of Zn^{2+} to a diatom [37] or to wheat roots [9].

Diffusive Gradients in Thin films (DGT) is based on the accumulation of metal in a disc of gel with embedded beads of Chelex resin, while another disc of gel serves to (practically) define the diffusion domain [38]. DGT has been applied to natural waters, sediments and soils [8, 39] and to hydroponic media [7, 40].

The Permeation Liquid Membrane (PLM) technique relies on the selective transportation of the analyte across a hydrophobic membrane via a carrier [41-43] and can be tuned to determine the free species (or to some labile fraction). Polymer Inclusion Membrane (PIM) is a membrane based technique where ion transfer requires binding to a carrier molecule [44], similarly to PLM, but much more robust. PIM have been recently shown to measure free ion concentrations [45].

The aim of the present work is to apply different techniques to determine the free (with AGNES and PIM) and labile fractions (with DGT and LASV) of Zn available in hydroponic medium at different concentrations of ligand (EDTA or humic acid). Zinc is an essential metal for plants (and its deficiency has been reported in soils of many arid regions of the world [7]), so its uptake attracts much attention. The relevant medium for plants is the soil solution, which can also be approximated by hydroponic media, much more controlled. Comparison of PIM, DGT and LASV results is performed by converting their respective responses to fluxes [40]. Special emphasis is devoted to the interpretation of the fluxes obtained with the dynamic speciation techniques.

2. Materials and Methods

2.1 Reagents

For the preparation of the nutrient solution the following reagents were used: $KNO_3 \cdot 4H_2O$, $Ca(NO_3)_2$, KH_2PO_4, $MgSO_4 \cdot 7H_2O$, NH_4NO_3, H_3BO_3, $MnCl_2 \cdot 4H_2O$, $CuSO_4 \cdot 5H_2O$, $Na_2MoO_4 \cdot 2H_2O$, $ZnSO_4 \cdot 7H_2O$; they were all purchased from Panreac (Barcelona, Spain). As an iron source, the commercial product Kelamix Fe was used (Sicosa, Girona, Spain). According to the producing company, 6% of the mass

corresponds to Fe, which is chelated by ethylenediamine-N,N'-bis(2-hydroxyphenylacetic acid) (EDDHA); but the complete formulation is undisclosed. The ESI-MS spectra of the product are shown in Fig SI-1. The buffer employed was 2-(N-morpholino) ethanesulfonic acid (MES) obtained from Fluka (Bern, Switzerland). Organic ligands such as humic acid sodium salt (technical grade, HA) and EDTA were provided by Sigma-Aldrich (St Louis, Missouri, USA). Elemental composition of HA, used as received, is presented in Table SI-1.

For PIM preparation, the polymer polyvinyl chloride (PVC) and the carrier di-2-ethylhexyl phosphoric acid (D2EHPA) were from Fluka (Bern, Switzerland) and Sigma-Aldrich (St Louis, Missouri, USA), respectively. Tetrahydrofuran (THF) solvent was from Panreac (Barcelona, Spain).

A standard solution 1000 mg L^{-1} Zn (Merck, Darmstadt, Germany) and solid KNO_3 (Fluka, St Louis, USA) TraceSelect grade were used to prepare the calibration standards for AGNES and LASV.

HNO_3 69% (Fisher Chemical, Loughborough, UK) was used for DGT elutions prior to ICP-MS analysis. A standard solution 1000 mg L^{-1} Zn (High Purity Standards, Charleston, USA) was used to prepare the calibration standards for ICP-MS.

All reagents and solvents used in this study were of analytical grade except the ones whose different quality has been specified.

Ultrapure water with 18 MΩ cm resistivity (Synergy UV purification system Millipore) was used in all preparations.

2.2 Preparation of hydroponic media

The nutrient solution was based on Hoagland growth medium [46]. The concentrations were modified by dilution to reach a final composition as follows: 2.5 mmol L^{-1} $KNO_3.4H_2O$, 2.5 mmol L^{-1} $Ca(NO_3)_2$, 0.25 mmol L^{-1} KH_2PO_4, 1 mmol L^{-1} $MgSO_4.7H_2O$, 0.5 mmol L^{-1} NH_4NO_3, 23 µmol L^{-1} H_3BO_3, 4.2 µmol L^{-1} $MnCl_2.4H_2O$, 0.1 µM $CuSO_4.5H_2O$, 0.25 µmol L^{-1} $Na_2MoO_4.2H_2O$, 0.38 µmol L^{-1} $ZnSO_4.7H_2O$, and 12 µmol L^{-1} Fe (from Kelamix). This solution composition is referred to as half-strength Hoagland medium. The pH was adjusted to 6.0±0.1 by using 2.5 mmol L^{-1} MES buffer. It has been reported that MES does not complex Zn significantly [47].

Different media have been considered in this work, with Zn added according to a previous work [45] and EDTA or HA concentrations to provide similar $[Zn^{2+}]$:

i. The control medium, with the composition detailed above.

ii. The control medium with an added Zn concentration: either 35.0 µmol L^{-1} (Zn_1) or 69.6 µmol L^{-1} (Zn_2), added as $ZnSO_4.7H_2O$.

iii. The medium with added Zn (35.0 µmol L^{-1} and 69.6 µmol L^{-1}), and also with the presence of 20 µmol L^{-1} EDTA (Zn+EDTA_1 and Zn+EDTA_2, respectively).

iv. The medium with added Zn (35.0 μmol L^{-1} and 69.6 μmol L^{-1}), and also with the presence of 60 mg L^{-1} humic acid (Zn+HA_1 and Zn+HA_2, respectively).

2.3 Experimental setups and instrumentation

PIMs containing 70% PVC and 30%D2EHPA were prepared using a procedure similar to that reported by Sugiura [48]. Briefly, 400 mg of PVC were weighted and dissolved in 12 mL of THF. After two hours stirring, one mL of the carrier solution, 0.5 mol L^{-1} D2EHPA in THF, was added to the mixture and stirred for 1 more hour. Finally, the resulting mixture was poured into a 9.0 cm diameter flat bottom glass petri dish, which was set horizontally and covered loosely. The organic solvent was allowed to evaporate over 24 h at room temperature, and the resulting film was carefully peeled off from the bottom of the petri dish. Circular pieces of 2 cm diameter were cut from the centre of the membrane and were, then, incorporated in a dedicated device, used as passive sampler [45]. The membrane device was partially immersed in 250 mL of the hydroponic solution under study, which was contained in a glass beaker placed on a magnetic stirrer, whereas 5 mL of 0.01 mol L^{-1} HNO_3 was used as acceptor phase. After a given contact time, the device was removed from the solution and the nitric acid solution was analyzed for total Zn content using a sequential inductively coupled plasma atomic emission spectrometer (ICP-AES) (Liberty RL, Varian, Mulgrave, Vic., Australia). PIM determinations were run at room temperature (23±1ºC).

AGNES and LASV voltammetric measurements were carried out with Eco Chemie Autolab PGSTAT101 and μAutolab Type III potentiostats attached to Metrohm 663VA

Stands being controlled from a computer by means of the NOVA 1.11 software. The working electrode was a Metrohm multimode mercury drop electrode. The smallest drop in our stand was chosen, which according to the catalogue corresponds to a radius around $r_0 = 1.41\times10^{-4}$ m. The auxiliary electrode was a glassy carbon electrode and the reference electrode was Ag/AgCl/3 mol L^{-1} KCl, encased in a jacket containing 0.1 mol L^{-1} KNO_3.

A glass combined electrode (Crison) was attached to an Orion Research 720A+ or to an Orion Dual Star ion analyzer (Thermo) and introduced in the cell to control the pH. A glass jacketed cell provided by Metrohm was used in all measurements. The vessel was thermostated at 25.0 °C.

DGT holders (piston type, 2 cm diameter window), polyacrylamide gel discs (diffusive disc, 0.8 mm thick, and Chelex resin disc, 0.4 mm thick) from DGT Research Ltd and cellulose nitrate membrane filters (0.45 μm Whatman) were used. DGT devices were prepared as described elsewhere[49]. The sensors have been left to equilibrate in a solution at the same pH and ionic strength as the sample (0.011 mol L^{-1} KNO_3 and 2.5 mmol L^{-1} MES) for at least 18 hours (see Supporting Information of ref. [49]). After that, the sensors have been deployed, for 24 and 48 h, inside a plastic bucket containing 2 L of medium kept at 240 rpm stirring rate and at 25.0ºC in a thermostated bath. Deployment solutions and metal accumulations (once eluted with HNO_3) in DGT experiments were analysed, in triplicate, with an ICP-MS 7700x (Agilent Technologies, Inc, Tokyo, Japan).

2.4 Procedures

2.4.1 Determination of free Zn concentrations with AGNES

AGNES consists in applying two stages [23, 29]: i) A first stage where we apply a deposition potential for a long enough time to reach Absence of Gradients in the concentration profiles and Nernstian Equilibrium at the electrode surface (these specific conditions are the main difference with other stripping techniques, like LASV); and ii) a second stage where we apply a reoxidation program and we measure the total charge or the diffusion-limited current after a certain time. In this work, we use the variant AGNES-I where the reoxidation program is a (constant) potential pulse under diffusion-limited conditions and we measure the current.

At the end of the first stage a preconcentration factor *Y* has been achieved

$$Y = \frac{[\mathrm{M}^0]}{[\mathrm{M}^{2+}]} = \exp\left[-\frac{2F}{RT}\left(E_1 - E^{0'}\right)\right] \qquad \text{Y(1)}$$

where *F* is the Faraday constant, *R* the gas constant, *T* the temperature, E_1 is the applied deposition potential and *E*º' the standard formal potential of the redox couple. *Y* is the gain in metal concentration across the surface due to its preconcentration in the amalgam following the application of E_1 and, in practise, is usually computed from the peak potential of an ancillary Differential Pulse Polarogram (DPP) with just metal and the background electrolyte.

The measurement of the faradaic current in the second stage allows the quantification of the free metal ion concentration

$$I_f = \eta Y \left[M^{2+} \right] \quad \text{If(2)}$$

where I_f is the faradaic current (obtained from the subtraction of the blank to the total current) and η is the normalised proportionality factor.

Prior to AGNES measurements, a calibration to obtain η is needed at the same ionic strength as the sample. The calibrations were performed at 0.011 M KNO_3 given the predictions of Visual MINTEQ [50] with the composition of the hydroponic medium described in Section 2.2.

The quantification of the free metal concentration in each hydroponic medium has been performed applying AGNES with two different *Y*-values as an extra checking. The *Y* ranged from 2 to 200 depending on the free concentration. For the control medium (the lowest free Zn concentration) *Y* of 100 and 200 were required. Only for this medium, to avoid large deposition times, AGNES with 2 Pulses in the deposition stage [51] was applied with $t_{1,a}$ = 70 s and $t_{1,b}$ =210 s (when preconcentrating to *Y*=100) or $t_{1,a}$=140 s and $t_{1,b}$=420 s (when aiming at *Y*=200). In all the cases, the waiting time at the desired gain (*Y*) without stirring was 50 s and the preconcentration factor applied in the stripping stage was 10^{-8}.

2.4.2 Determination of labile fluxes with LASV using linear stripping scan

Essentially, LASV technique provides an accumulation resulting from the flux of analyte under diffusion-limited conditions acting throughout the deposition time. Indeed, the very

negative potential during the deposition stage creates a flux, due to the reduction -at the electrode surface- of Zn^{2+} (resulting directly from the free Zn flux or from the diffusion and dissociation of labile complexes). Steady state can be assumed during this deposition stage due to the vigorous stirring in the electrochemical cell and the short life of the transient regime. The linear stripping scan quantifies the amount of Zn^o accumulated in the amalgam (which corresponds to the steady-state accumulation during the deposition stage plus a small amount of Zn^o accumulated at the beginning of the linear stripping scan, when the stripping potential is still close to the deposition one, before Zn^o re-oxidation starts), without further complications (as in the Differential Pulse mode, where repeated oxidation/reduction cycles are much more difficult to interpret). The interfering impact of adsorption (e.g. humic acid complexes on the electrode surface) on the final stripped charge in this variant of LASV is expected to be mild, because diffusion-limited conditions in the deposition stage hinder electrodic adsorption [52] and any possible adsorption along the stripping step might distort a transient intensity current, but not the final charge (that, due to Faraday law, has to be proportional to the total accumulated concentration of Zn^o).

In the first stage of the LASV experiment, a deposition potential of -1.3V is applied during 60 s, followed -in the second stage- by a linear scan from -1.3V to 0 V at a scan rate of 0.0198 V s^{-1}(v) which produces a peak in the I vs E representation. The area of the peak is measured and allows the determination of the flux (J) as

$$J = \frac{Q}{2\,F\,A\,t} = \frac{Area_{\mathrm{LASVpeak}}}{v2FAt} \qquad \text{J(3)}$$

where Q is the charge (corresponding to the moles of reoxidated metal) which can be obtained from the peak area $Area_{LASVpeak}$ and the scan rate (v). A is the surface area of the mercury electrode (0.25 mm^2) and t is the deposition time.

2.4.3 Determination of labile fluxes with DGT

Under the assumption of steady-state regime along the deployment time (which will be checked for the hydroponic systems), the flux (J) can be computed from the number of (measured) accumulated moles of analyte in the resin disc, n_{Zn}, with the expression [53]:

$$J = \frac{n_{Zn}}{A\,t} \qquad \text{FluxDGT(4)}$$

where A is the area of the opening (3.14 cm^2) and t the deployment time.

In many works, the accumulation of the analyte into the binding phase is associated with a labile fraction or the so-called DGT-concentration c_{DGT} [53] assuming a steady-state regime under diffusion-limited conditions:

$$J = \frac{D_M c_{DGT}}{\delta^g} \qquad \text{J(5)}$$

where D_M is the diffusion coefficient of the metal analyte and δ^g is the thickness of the diffusion domain (usually the aggregate thickness of disc gel, filter and diffusive boundary layer).

2.4.4 Determination of free concentration with PIM

The PIM technique is based on carrier-mediated transport of the metal across the polymeric membrane. The carrier, D2EHPA in this case, forms a neutral complex with the Zn^{2+} ion at the membrane/donor interface. Then, the complex diffuses across the membrane, and when reaching the membrane/acceptor interface, the metal is released into the acceptor phase due to the protonation of the carrier in the aqueous phase with existing HNO_3. This chemical pumping allows the accumulation of the analyte in the acceptor solution. Recent work [45] has proposed that there is a co-limitation by transport both across the membrane and in the acceptor solution (rather than a limitation by diffusion in the source solution), leading to an accumulation proportional to the free ion concentration in the source solution, analogously to some cases of the PLM technique.

3. Results and discussion

3.1 Free concentration and fluxes provided by each technique

The free Zn concentration in the different hydroponic media considered in this work has been determined with AGNES (see Fig fig_AGNES 1 or Table SI-2), using the parameters detailed in section 2.4.1. The $[Zn^{2+}]$ found in the control medium, 0.111 μmol L^{-1}, is negligible in front of the free concentrations in media with spiked Zn. As expected, the free Zn concentration increases when increasing the total metal concentration of the medium (compare full and empty blue square markers in Fig fig_AGNES 1), while the free Zn concentration decreases with the addition of a ligand like EDTA (red triangles) or humic acid (green circles). For the conditions and concentrations considered in this work, 60 mg L^{-1} humic acid (equivalent to a concentration of sites of 342 μmol L^{-1},

316 according to the generic parameters of the NICA-Donnan model [54]) binds less Zn than
317 20 μmol L^{-1} EDTA, given the found lower free Zn concentrations in the EDTA-enriched
318 solutions.

319

320 For the sake of simplicity, when quantifying the contribution of the different complexes,
321 one can consider that the Hoagland medium acts as an equivalent ligand (labelled "Hoag")
322 to form an effective 1:1 complex labelled "MHoag". We neglect any variation of the
323 effective free ligand due to its complexation with the metal (the so-called ligand excess
324 conditions), so that

325 $$c_{\mathrm{M\,Hoag}} \approx K' c_{\mathrm{M}} \qquad \text{KPrime(6)}$$

326 where *K*' is the excess (conditional) stability constant (or stability coefficient). The mass
327 balance (when other complexes are still not added) can be written as

328 $$c_{\mathrm{T,M}} = c_{\mathrm{M}} + c_{\mathrm{M\,Hoag}} = \left(1 + K'\right) c_{\mathrm{M}} \qquad \text{Balance(7)}$$

329 *K*' has been evaluated as 0.21 ± 0.06 from the regression of the data (free and total) of
330 AGNES experiments with the control and with just added Zn (i.e. Zn_1 and Zn_2), while
331 also forcing the regression to pass through the origin. Using only one *K*' for the Hoagland
332 mixture is valid, for exemple, when the free concentrations of all participating ligands
333 (including EDDHA not bound to Fe) are constant despite Zn complexation. The linearity
334 observed in the plot $c_{\mathrm{T,M}}$ vs c_{M} lends support to the use of just one *K*' as a first
335 approximation to describe the binding properties of the Hoagland medium.

336

337 Fluxes recorded with LASV followed a similar pattern to the concentrations measured
338 with AGNES (see Table SI-2 in Supporting Information, and Fig Fig_ASV_systems2):

lower fluxes for lower total concentrations or solutions with an added ligand. The flux computed with eqn. (3) from the LASV peak area measured in the control medium was 10.3 nmol $m^{-2}s^{-1}$. The flux of Zn_2 is approximately twice that of Zn_1, consistent with the approximation of labile complexation with the Hoagland medium. The decrease (with respect to fluxes of Zn_1 and Zn_2) due to EDTA addition is similar for both total Zn concentrations, as expected for a formed strong inert complex. The impact of EDTA in reducing the analytical signal is, again, more important than that of humic acid.

For DGT, the accumulations were measured after 24 and 48 h. The almost direct proportionality between accumulation and deployment time seen in Fig. fig_DGT3 indicates that the system is under steady-state regime. Under these conditions, equation (4) can be applied to compute the flux. DGT fluxes follow a similar trend to the free concentrations measured with AGNES: the presence of EDTA or HA reduce the accumulation (for a given time) as seen in Fig. fig_DGT3. The reduction of the flux due to the addition of a ligand can be understood as due to a partial complexation of the Zn ions, leading to a reduced availability (compared with that resulting if the total concentration of Zn was free). This decrease in availability can be due to a much lower diffusion coefficient of the complex (the expected case for a macromolecular entity like humic acid diffusing in a gel), due to a lower lability degree (the expected case for EDTA), as described below in section 3.2 or due to a combination of both effects. From the point of view of DGT, the fluxes with EDTA and HA have essentially the same value (within experimental error) which is compatible with the diffusion coefficient of ZnHA being smaller than that of ZnEDTA.

As with DGT technique, the direct proportionality between accumulation and deployment time seen in Fig. SI-2 for PIM experiments indicates that the system is under steady-state regime and can be computed with using equation (4). PIM fluxes due to ligand additions can be seen in Fig. fig_PIM_systems4 and can be interpreted along the lines of the previous paragraph. In agreement with the measurements of the other techniques, J_{PIM} decreases when EDTA is added, as expected for the formation of a complex, and remains below J_{PIM} corresponding to the system with HA. Moreover, the declines in the computed fluxes due to the addition of EDTA or humic acid are similar to those seen with AGNES, LASV and DGT.

3.2. Relationship between the information provided by different techniques

The interpretative framework developed for DGT (see, for instance [53]) can be extended to other techniques yielding fluxes. A key idea is to split the total flux of metal into the contribution from the free metal (J_{free}, represented as dotted lines in Figs. fig_DGT_AGNES5-fig_SV_AGNES6) plus the contribution from the complexes. These complexes can be classified as those complexes existing in the Hoagland medium and those complexes due to a ligand addition (EDTA and HA), with the general label ML:

$$J = J_{total} = J_{free} + J_{Hoag} + J_{ML} = \frac{D_M}{\delta} c_M + \frac{D_{Hoag}}{\delta} c_{M\,Hoag} \xi_{Hoag} + \frac{D_{ML}}{\delta} c_{ML} \xi_{ML} \qquad \text{Flux(8)}$$

where D_i is the diffusion coefficient of the species (free metal, M; complex with the medium MHoag; complex with added ligand, ML), c_i is the concentration of each species, ξ_i is the lability degree of each species (see Introduction), and δ is the thickness of the diffusion layer of the technique. In DGT, δ corresponds to the summation of gel, filter and Diffusive Boundary Layer thicknesses, while in LASV δ will depend on the

stirring rate with no fixed term. If one considers δ an operational parameter to reproduce fluxes in well defined hydrodynamic regimes (such as laminar flow), it will depend on (some powers of) the diffusion coefficients of the participating species [55, 56]. However, turbulence (or natural convection due to local inhomogeneities in temperature o density of solution) renders the consideration of laminar flow also approximate, supporting the rough first approximation of considering δ as fixed. This is the satisfactory standard approach to deal with the DBL in DGT [57]. For PIM, eqn. Flux(8) would apply if the limiting step was diffusion in the solution. On the other hand, if the liming step is not diffusion in the solution, then the flux does not contain any information on the lability or amount of complexes in the sample, but just on the free metal ion[45].

Given that the ligands of the Hoagland medium are not macromolecular, one can assume $D_{\mathrm{Hoag}}=D_{\mathrm{M}}$. As the expected (inorganic) complexes of Zn with the medium are weak, one can assume that they are fully labile, so $\xi_{\mathrm{Hoag}}=1$. Combining eqns. Flux(8) and (7):

$$J = \frac{D_{\mathrm{M}}}{\delta}\left(1+K'\right)c_{\mathrm{M}} + \frac{D_{\mathrm{ML}}}{\delta}c_{\mathrm{ML}}\xi_{\mathrm{ML}} \qquad \text{FluxGeneral(9)}$$

From the particular case of experiments Zn_1 and Zn_2 (i.e. when $c_{\mathrm{ML}}=0$), one can compute D_{M}/δ which could be called the flux factor

$$\frac{D_{\mathrm{M}}}{\delta} = \frac{J}{c_{\mathrm{M}}\left(1+K'\right)} = \frac{J}{c_{\mathrm{T,M}}} \qquad \text{FactorFlux(10)}$$

For DGT, the experimentally retrieved flux factor (0.52×10^{-6} m s^{-1}) is close to the theoretical one (0.55×10^{-6} m s^{-1}) computed from $D_{Zn}=6.08\times10^{-10}$ m^2s^{-1} for Zn diffusion in the gel (from DGT research website) and δ=1.1 mm. For LASV, $(D_M/\delta)_{exp}=3.4\times10^{-5}$ m s^{-1} while $(D_M/\delta)_{theor}=3.6\times10^{-5}$ m s^{-1} (taking $\delta_{LASV}=2\times10^{-5}$ m [23, 58, 59] and $D_{Zn}=7.3\times10^{-10}$ m^2s^{-1} for Zn diffusion in water).

According to equation FluxGeneral(9), a representation of the flux in terms of the free metal concentration, for solutions where the second term was negligible, would yield a straight line passing through the origin. Such a "medium line" can be drawn from the experimental flux factor of each technique and the obtained *K*' (see brown continuous lines in Figs. fig_DGT_AGNES5-fig_SV_AGNES6). These lines should go through markers corresponding to Zn_1 and Zn_2 (square blue markers), which is approximately the case in Figs. fig_DGT_AGNES5-fig_SV_AGNES6.

The ordinate difference between any of the rest of experimental markers and this brown continuous line can be called "offset" and physically corresponds to the contribution to the flux of the complex (other than the complexes with the medium, MHoag) expressed by the last term in eqn. FluxGeneral(9):

$$J_{ML} = \xi_{ML}\frac{D_{ML}c_{ML}}{\delta} \qquad \text{(offset(11)}$$

For cases with an added ligand, the lability degree can be computed from the corresponding offset of the marker with respect to the medium line (brown continuous line), just by solving for ξ_{ML} in eqn (11) and taking c_{ML} as:

$$c_{\mathrm{ML}} = c_{\mathrm{T,M}} - c_{\mathrm{M}}\left(1 + K'\right) \qquad \text{defY(12)}$$

In the technique DGT, see Fig fig_DGT_AGNES5, EDTA offsets can be converted into lability degrees by assuming D_{ML}=D_{M}. For the low Zn concentration, one finds ξ_{EDTA}=0.31, while for the higher concentration ξ_{EDTA}=0.60. The difference has to be mostly ascribed to experimental errors and inaccuracies in the input parameters (total concentrations, free concentration, *K*', DGT fluxes, etc.) required for the calculations. Indeed, as most of the analytical signal (i.e. the flux) comes from the free Zn concentration, the small difference between the total and this free contribution (i.e. the offset) accumulates (relatively) large uncertainties. The key conclusion is a rather low ξ_{EDTA}, consistent with the inert nature of ZnEDTA, but it could also be consistent with an insufficient effective affinity of Zn for the iminodiacetic resin (of the Chelex resin used in our DGT) in front of the strong ligand (EDTA), see [60, 61].

To extract lability degrees for HA complexes from the offsets, we take D_{M}=D_{Zn}=6.08×10^{-10} m^{2}s^{-1} and D_{ML}=4.77×10^{-10} m^{2}s^{-1} (average value of the range reported recently [62]) which lead to a ratio D_{ML}/D_{M}=0.78.

For the probed HA solutions with DGT, Fig fig_DGT_AGNES5, assuming D_{ML}=0.78×D_{M}, the offsets translate to ξ_{HA}=0.10 for Zn+HA_1 and ξ_{HA}=0.99 for Zn+HA_2, respectively. The increase of the lability degree of humic acid when the Zn concentration increases can be understood due to the increasing occupation by Zn ions of humic sites with decreasing affinity. Assuming Eigen's complexation mechanism [63], a

decrease in the affinity of a site can be ascribed to an increase of the dissociation rate constant, increasing in this way the lability. For the higher concentration of the present work, ξ_{HA} is higher than for EDTA, in broad agreement with some quite labile behaviour reported for Zn complexes with humic acids [64]. Notice that the knowledge of the diffusion coefficient value is necessary to compute the lability degree. In this regard, an equation previously used in the literature, eqn (7) in [5] and eqn. (6) in [9] would not be valid for a complex with a diffusion coefficient different from that of the metal (as it is the case with HA). The equation can be corrected as follows:

$$\xi_{ML} = \left(\frac{J}{J_{free}} - 1 \right) \frac{c_M}{D_{ML} c_{ML}} \qquad \text{Degryse(13)}$$

where J_{free} is the flux obtained in a system which has only metal and whose free concentration is just the same as in the solution where there is also the complex. This equation is not applied in this work because this special solution with just metal has not been prepared.

For the technique LASV, triangle markers in Fig fig_SV_AGNES6 reflect a positive offset for Zn+EDTA_1, while for the higher concentration, the offset is negative. As both are of the same order of magnitude, and considering that a negative offset renders meaningless any computation with Eqn. ((11), we can conclude that the lability degree of ZnEDTA is close to zero for this technique. The offsets for HA are too disperse to be subject to a qualitative mathematical analysis. We speculate that perhaps a low reproducibility of stirring between days (which impacts on the thickness of the diffusion layer) might be responsible for an accuracy insufficient for the low ligand to metal ratio of these experiments.

One can highlight that the lability degree of a complex is not an intrinsic property of the complex, but it is also sensor and technique dependent. Actually, the lability depends not only on the ability of the complex to dissociate (dissociation rate constant, composition of the media), but also on the spatial and time scale where this dissociation takes place (e.g. the characteristics of the sensor) [65].

A well-known effect is that lability increases when the thickness of the diffusion layer increases [33, 65]. Thus, one expects that lability degrees measured by DGT are higher than those measured by LASV in the same chemical system, because the main difference between both techniques is the thickness of the diffusion layer (of the order of 1.1 mm for DGT and just 20 μm for LASV [58]). Additionally, the penetration of complexes in the resin disc, where free metal is absent and dissociation proceeds, renders them more labile in DGT [66, 67]. Although this is the trend of ξ values obtained above for EDTA, unfortunately, they do not allow a clear confirmation of this expectation. In this respect, DGT computations of the lability degree are more trustable, because of the smaller variation between experiments and a better defined value of δ in the technique.

In the PIM technique, eqn. Flux(8) does not apply, because the flux is not determined by diffusion in the solution [45]. So, with PIM -despite measuring a flux - no information on the lability of the complexes in the solution can be gained. Fig fig_PIM_AGNES7 confirms -within the experimental error- the proportionality between PIM fluxes and the measurements of free Zn concentrations provided by AGNES. This is expected from PIM fluxes being proportional to the free Zn concentration [45].

If we compare now directly the results between techniques, we observe that DGT and LASV are very well correlated (see Fig fig_DGT_SV8). The LASV fluxes also correlate well with PIM fluxes (see Fig SI-3). These correlations can be attributed to the low ligand to metal ratio used in these experiments.

4. Conclusions

Equation FluxGeneral(9) supports the representation (seen in Figs fig_DGT_AGNES5, and fig_SV_AGNES6) of the fluxes in front of the free ion concentration (provided by AGNES or PIM). The last term in Equation FluxGeneral(9) is visualized as the distance (or offset) between a marker and the line corresponding to the contribution of the fixed ligands of the medium. From this last term, lability degree can be computed, though more work is needed to obtain more reliable estimates. Those lability degrees derived here from DGT measurement are the most robust, probably because of the better controlled thickness of the diffusion layer.

The results from this work (see Fig fig_PIM_AGNES7) confirm that, in these conditions, PIM can be used to measure free metal ion concentrations. So, plots like Figs fig_DGT_AGNES5 and fig_SV_AGNES6 could also be drawn taking as abscissae the values of the PIM fluxes (or its conversion into free concentrations via a calibration) instead of AGNES free concentrations.

In principle, the different techniques provide access to different fractions of the analyzed system and their information can be considered as complementary [32]. However, for some conditions, the differences might be not large enough to be quantified. This leads to a kind of equivalence of the techniques (for such systems) which results in more robust and confirmed conclusions when there is general agreement between them. Due to this equivalence (under the present conditions this might be related to a relative large proportion of free Zn in comparison with the complexed forms), other criteria for selecting a technique can be adopted. For instance, the application of LASV with the mercury electrode has the advantage of the reduced time of the experiment when compared with DGT and PIM. LASV does not requires the analysis with a complementary technique (ICP-MS or ICP-OES). On the other hand, DGT and PIM can be applied *in situ*, which avoids contaminations in sampling and storage (though there is also a transport of the accumulated analyte towards the laboratory for an instrumental analysis).

The found correlations between the assayed techniques also suggests that in some systems, like the one shown here, a correlation between the results of one technique with a particular plant uptake or toxicity might not be proof of the free metal or a given labile fraction being their relevant determinant.

Acknowledgements

This work was financially supported by the Spanish Ministry of Education and Science (projects CTM2013-48967 and CTM2016-78798). Alexandra Altier's help with DGT experiments is acknowledged.

Supplementary data

Electronic supplementary information related to this article can be found at http://dx.doi.org/XXXXX.

Literature cited

1. M. A. Anderson, F. M. M. Morel, R. R. L. Guillard, Growth limitation of a coastal diatom by low zinc ion activity, Nature, 276 (1978) 70-71.

2. P. R. Paquin, J. W. Gorsuch, S. Apte, G. E. Batley, K. C. Bowles, P. G. C. Campbell, C. G. Delos, D. M. Di Toro, R. L. Dwyer, F. Galvez, R. W. Gensemer, G. G. Goss, C. Hogstrand, C. R. Janssen, J. C. McGeer, R. B. Naddy, R. C. Playle, R. C. Santore, U. Schneider, W. A. Stubblefield, C. M. Wood, K. B. Wu, The biotic ligand model: a historical overview, Comp. Biochem. Physiol. C, 133 (2002) 3-35.

3. A. Larbi, F. Morales, A. Abadia, Y. Gogorcena, J. J. Lucena, J. Abadia, Effects of Cd and Pb in sugar beet plants grown in nutrient solution: induced Fe deficiency and growth inhibition, Functional Plant Biology, 29 (2002) 1453-1464.

4. C. M. Zhao, P. G. C. Campbell, K. J. Wilkinson, When are metal complexes bioavailable?, Environ. Chem., 13 (2016) 425-433.

5. F. Degryse, E. Smolders, D. R. Parker, Metal complexes increase uptake of Zn and Cu by plants: implications for uptake and deficiency studies in chelator-buffered solutions, Plant Soil, 289 (2006) 171-185.

6. F. Degryse, E. Smolders, R. Merckx, Labile Cd complexes increase Cd availability to plants, Environ. Sci. Technol., 40 (2006) 830-836.

7. A. Gramlich, S. Tandy, E. Frossard, J. Eikenberg, R. Schulin, Diffusive limitation of zinc fluxes intro wheat roots, PLM and DGT devices in the presence of organic ligands, Environ. Chem., 11 (2014) 41-50.

8. J. Luo, H. Zhang, F. J. Zhao, W. Davison, Distinguishing Diffusional and Plant Control of Cd and Ni Uptake by Hyperaccumulator and Nonhyperaccumulator Plants, Environmental Science & Technology, 44 (2010) 6636-6641.

9. P. Wang, D. M. Zhou, X. S. Luo, L. Z. Li, Effects of Zn-complexes on zinc uptake by wheat (Triticum aestivum) roots: a comprehensive consideration of physical, chemical and biological processes on biouptake, Plant Soil, 316 (2009) 177-192.

10. R. Albajes, C. Cantero-Martinez, T. Capell, P. Christou, A. Farre, J. Galceran, F. López-Gatius, S. Marin, O. Martin-Belloso, M. J. Motilva, C. Nogareda, J. Peman, J. Puy, J. Recasens, I. Romagosa, M. P. Romero, V. Sanchis, R. Savin, G. A. Slafer, R. Soliva-Fortuny, I. Viñas, J. Voltas, Building bridges: an integrated strategy for sustainable food production throughout the value chain, Molecular Breeding, 32 (2013) 743-770.

11. P. Bradac, R. Behra, L. Sigg, Accumulation of Cadmium in Periphyton under Various Freshwater Speciation Conditions, Environmental Science & Technology, 43 (2009) 7291-7296.

12. A. M. Mota, J. P. Pinheiro, M. L. S. Goncalves, Electrochemical Methods for Speciation of Trace Elements in Marine Waters. Dynamic Aspects, J. Phys. Chem. A, 116 (2012) 6433-6442.

13. F. Degryse, E. Smolders, H. Zhang, W. Davison, Predicting availability of mineral elements to plants with the DGT technique: a review of experimental data and interpretation by modelling, Environ. Chem., 6 (2009) 198-218.

14. J. H. Ren, P. N. Williams, J. Luo, H. R. Ma, X. R. Wang, Sediment metal bioavailability in Lake Taihu, China: evaluation of sequential extraction, DGT, and PBET techniques, Environ. Sci. Pollut. R., 22 (2015) 12919-12928.

15. A. Gramlich, S. Tandy, C. Gauggel, M. Lopez, D. Perla, V. Gonzalez, R. Schulin, Soil cadmium uptake by cocoa in Honduras, Sci. Total Envir., 612 (2018) 370-378.

16. M. Pesavento, G. Alberti, R. Biesuz, Analytical methods for determination of free metal ion concentration, labile species fraction and metal complexation capacity of environmental waters: A review, Anal. Chim. Acta, 631 (2009) 129-141.

17. J. Feldmann, P. Salaun, E. Lombi, Critical review perspective: elemental speciation analysis methods in environmental chemistry - moving towards methodological integration, Environ. Chem., 6 (2009) 275-289.

18. R. F. Domingos, A. Gelabert, S. Carreira, A. Cordeiro, Y. Sivry, M. F. Benedetti, Metals in the Aquatic Environment-Interactions and Implications for the Speciation and Bioavailability: A Critical Overview, Aquat. Geochem., 21 (2015) 231-257.

19. E. Companys, J. Galceran, J. P. Pinheiro, J. Puy, P. Salaün, A review on electrochemical methods for trace metal speciation in environmental media, Current Opinion in Electrochemistry, 3 (2017) 144-162.

20. E. Bakker, E. Pretsch, Modern Potentiometry, Angew. Chem. , Int. Ed., 46 (2007) 5660-5668.

21. E. J. M. Temminghoff, A. C. C. Plette, R. van Eck, W. H. van Riemsdijk, Determination of the chemical speciation of trace metals in aqueous systems by the Wageningen Donnan Membrane Technique, Anal. Chim. Acta, 417 (2000) 149-157.

22. C. Fortin, F. Caron, Complexing capacity of low-level radioactive waste leachates for Co-60 and Cd-109 using an ion-exchange technique, Anal. Chim. Acta, 410 (2000) 107-117.

23. J. Galceran, E. Companys, J. Puy, J. Cecília, J. L. Garcés, AGNES: a new electroanalytical technique for measuring free metal ion concentration, J. Electroanal. Chem., 566 (2004) 95-109.

24. D. Chito, L. Weng, J. Galceran, E. Companys, J. Puy, W. H. van Riemsdijk, H. P. van Leeuwen, Determination of free Zn^{2+} concentration in synthetic and natural samples with AGNES (Absence of Gradients and Nernstian Equilibrium Stripping) and DMT (Donnan Membrane Technique), Sci. Total Envir., 421-422 (2012) 238-244.

25. C. Parat, L. Authier, A. Castetbon, D. Aguilar, E. Companys, J. Puy, J. Galceran, M. Potin-Gautier, Free Zn^{2+} determination in natural freshwaters of the Pyrenees: towards on-site measurements with AGNES, Environ. Chem., 12 (2015) 329-337.

629 26. H. B. C. Pearson, J. Galceran, E. Companys, C. Braungardt, P. Worsfold, J. Puy, S.
630 Comber, Absence of Gradients and Nernstian Equilibrium Stripping (AGNES) for
631 the determination of [Zn2+] in estuarine waters, Anal. Chim. Acta, 912 (2016) 32-
632 40.

633 27. J. Galceran, C. Huidobro, E. Companys, G. Alberti, AGNES: a technique for
634 determining the concentration of free metal ions. The case of Zn(II) in coastal
635 Mediterranean seawater., Talanta, 71 (2007) 1795-1803.

636 28. C. David, J. Galceran, C. Rey-Castro, J. Puy, E. Companys, J. Salvador, J. Monné,
637 R. Wallace, A. Vakourov, Dissolution kinetics and solubility of ZnO nanoparticles
638 followed by AGNES., J. Phys. Chem. C, 116 (2012) 11758-11767.

639 29. J. Galceran, M. Lao, C. David, E. Companys, C. Rey-Castro, J. Salvador, J. Puy,
640 The impact of electrodic adsorption on Zn, Cd or Pb speciation measurements with
641 AGNES, J. Electroanal. Chem., 722-723 (2014) 110-118.

642 30. E. Companys, M. Naval-Sanchez, N. Martinez-Micaelo, J. Puy, J. Galceran,
643 Measurement of free zinc concentration in wine with AGNES, J. Agric. Food
644 Chem., 56 (2008) 8296-8302.

645 31. G. Alberti, R. Biesuz, C. Huidobro, E. Companys, J. Puy, J. Galceran, A comparison
646 between the determination of free Pb(II) by two techniques: Absence of Gradients
647 and Nernstian Equilibrium Stripping and Resin Titration, Anal. Chim. Acta, 599
648 (2007) 41-50.

649 32. L. Sigg, F. Black, J. Buffle, J. Cao, R. Cleven, W. Davison, J. Galceran, P. Gunkel,
650 E. Kalis, D. Kistler, M. Martin, S. Noel, Y. Nur, N. Odzak, J. Puy, W. H. van
651 Riemsdijk, E. Temminghoff, M. L. Tercier-Waeber, S. Toepperwien, R. M. Town,
652 E. Unsworth, K. W. Warnken, L. P. Weng, H. B. Xue, H. Zhang, Comparison of
653 analytical techniques for dynamic trace metal speciation in natural freshwaters,
654 Environ. Sci. Technol., 40 (2006) 1934-1941.

655 33. J. Galceran, J. Puy, J. Salvador, J. Cecília, H. P. van Leeuwen, Voltammetric lability
656 of metal complexes at spherical microelectrodes with various radii, J. Electroanal.
657 Chem., 505 (2001) 85-94.

658 34. J. Puy, J. Galceran, Theoretical aspects of dynamic metal speciation with
659 electrochemical techniques, Current Opinion in Electrochemistry, 1 (2017) 80-87.

660 35. G. E. Batley, S. C. Apte, J. L. Stauber, Speciation and bioavailability of trace metals
661 in water: Progress since 1982, Aust. J. Chem., 57 (2004) 903-919.

662 36. O. M. Lage, H. M. V. M. Soares, M. T. S. D. Vasconcelos, A. M. Parente, R.
663 Salema, Toxicity effects of copper(II) on the marine dinoflagellate Amphidinium
664 carterae: Influence of metal speciation, Eur. J. Phycol., 31 (1996) 341-348.

665 37. J. M. Kim, O. Baars, F. M. M. Morel, The effect of acidification on the
666 bioavailability and electrochemical lability of zinc in seawater, Philosophical
667 Transactions of the Royal Society A-Mathematical Physical and Engineering
668 Sciences, 374 (2016).

669 38. W. Davison, H. Zhang, In-situ speciation measurements of trace components in
670 natural- waters using thin-film gels, Nature, 367 (1994) 546-548.

671 39. A. A. Menegario, L. N. M. Yabuki, K. S. Luko, P. N. Williams, D. M. Blackburn,
672 Use of diffusive gradient in thin films for in situ measurements: A review on the
673 progress in chemical fractionation, speciation and bioavailability of metals in
674 waters, Anal. Chim. Acta, 983 (2017) 54-66.

675 40. M. Jakl, J. J. Dytrtova, D. Miholova, D. Kolihova, J. Szakova, P. Tlustos, Passive
676 diffusion assessment of cadmium and lead accumulation by plants in hydroponic
677 systems, Chemical Speciation and Bioavailability, 21 (2009) 111-120.

678 41. N. Parthasarathy, J. Buffle, Capabilities of supported liquid membranes for metal
679 speciation in natural-waters - application to copper speciation, Anal. Chim. Acta,
680 284 (1994) 649-659.

681 42. L. Tomaszewski, J. Buffle, J. Galceran, Theoretical and analytical characterisation
682 of a flow-through permeation liquid membrane with well-controlled flux for metal
683 speciation measurements, Anal. Chem., 75 (2003) 893-900.

684 43. A. Gramlich, S. Tandy, V. I. Slaveykova, A. Duffner, R. Schulin, The use of
685 permeation liquid membranes for free zinc measurements in aqueous solution,
686 Environ. Chem., 9 (2012) 429-437.

687 44. R. Guell, E. Antico, S. D. Kolev, J. Benavente, V. Salvado, C. Fontas, Development
688 and characterization of polymer inclusion membranes for the separation and
689 speciation of inorganic As species, J. Membrane Sci., 383 (2011) 88-95.

690 45. R. Vera, C. Fontàs, J. Galceran, O. Serra, E. Anticó, Polymer inclusion membrane
691 to access Zn speciation: Comparison with root uptake, Sci. Total Envir., 622–623
692 (2018) 316-324.

693 46. D. R. Hoagland, D. I. Arnon, University of California, College of Agriculture,
694 Agricultural Experiment Station., Berkeley, CA (USA), 1950.

695 47. H. M. V. M. Soares, S. C. Pinho, M. G. R. T. M. Barros, Influence of N-Substituted
696 Aminosulfonic Acids with a Morpholinic Ring pH Buffers on the Redox Processes
697 of Copper or Zinc Ions: A Contribution to Speciation Studies, Electroanal., 11
698 (1999) 1312-1317.

699 48. M. Sugiura, Transport of Lanthanide lons through Cellulose Triacetate Membranes
700 Containing Hinokitiol and Flavonol as Carriers, Sep. Sci. Technol., 25 (1990) 1189-
701 1199.

702 49. J. Puy, J. Galceran, S. Cruz-Gonzalez, C. A. David, R. Uribe, C. Lin, H. Zhang, W.
703 Davison, Metal accumulation in DGT: Impact of ionic strength and kinetics of
704 dissociation of complexes in the resin domain, Anal. Chem., 86 (2014) 7740-7748.

705 50. Gustafsson, J. P.Visual MINTEQ version 3.0. <www.lwr.kth.se/English/
706 Oursoftware/vminteq/index.htm> 2010

707 51. E. Companys, J. Cecília, G. Codina, J. Puy, J. Galceran, Determination of the
708 concentration of free Zn^{2+} with AGNES using different strategies to reduce the
709 deposition time., J. Electroanal. Chem., 576 (2005) 21-32.

710 52. J. Galceran, D. Rene, J. Salvador, J. Puy, M. Esteban, F. Mas, Reverse Pulse
711 Polarography of labile metal + macromolecule systems with induced reactant
712 adsorption - Theoretical analysis and determination of domplexation and adsorption
713 parameters, J. Electroanal. Chem., 375 (1994) 307-318.

714 53. J. Galceran, J. Puy, Interpretation of diffusion gradients in thin films (DGT)
715 measurements: a systematic approach, Environ. Chem., 12 (2015) 112-122.

716 54. C. J. Milne, D. G. Kinniburgh, W. H. van Riemsdijk, E. Tipping, Generic NICA-
717 Donnan model parameters for metal-ion binding by humic substances, Environ. Sci.
718 Technol., 37 (2003) 958-971.

719 55. H. P. van Leeuwen, J. Galceran, in H.P.van Leeuwen, W.Koester (Eds.),
720 Physicochemical kinetics and transport at chemical-biological surfaces, vol. 9, John
721 Wiley, Chichester, UK, 2004, Ch.3.

722 56. J. P. Pinheiro, H. P. van Leeuwen, Metal speciation dynamics and bioavailability.
723 2. Radial diffusion effects in the microorganism range, Environ. Sci. Technol., 35
724 (2001) 894-900.

725 57. K. W. Warnken, W. Davison, H. Zhang, J. Galceran, J. Puy, In situ measurements
726 of metal complex exchange kinetics in freshwater, Environ. Sci. Technol., 41 (2007)
727 3179-3185.

728 58. M. G. Bugarin, A. M. Mota, J. P. Pinheiro, ML. S. Gonçalves, Influence of metal
729 concentration at the electrode surface in Differential-Pulse Anodic-Stripping
730 Voltammetry in the presence of humic matter, Anal. Chim. Acta, 294 (1994) 271-
731 281.

732 59. R. M. Town, H. P. van Leeuwen, Fundamental features of metal ion determination
733 by stripping chronopotentiometry, J. Electroanal. Chem., 509 (2001) 58-65.

734 60. S. Mongin, R. Uribe, C. Rey-Castro, J. Cecilia, J. Galceran, J. Puy, Limits of the
735 Linear Accumulation Regime of DGT Sensors, Environ. Sci. Technol., 47 (2013)
736 10438-10445.

737 61. J. Puy, J. Galceran, C. Rey-Castro, in W.Davison (Ed.), Diffusive Gradients in Thin-
738 Films for Environmental Measurements, Cambridge University Press, Cambridge,
739 2016, Ch.5.

740 62. J. Balch, C. Gueguen, Effects of molecular weight on the diffusion coefficient of
741 aquatic dissolved organic matter and humic substances, Chemosphere, 119 (2015)
742 498-503.

743 63. M. Eigen, R. Wilkins, The Kinetics and Mechanism of Formation of Metal
744 Complexes, 49 ed., American Chemical Society, Washington, 1965.

745 64. E. Companys, J. Puy, J. Galceran, Humic acid complexation to Zn and Cd
746 determined with the new electroanalytical technique AGNES, Environ. Chem., 4
747 (2007) 347-354.

748 65. H. P. van Leeuwen, R. M. Town, J. Buffle, R. Cleven, W. Davison, J. Puy, W. H.
749 van Riemsdijk, L. Sigg, Dynamic speciation analysis and Bioavailability of metals
750 in Aquatic Systems, Environ. Sci. Technol., 39 (2005) 8545-8585.

751 66. S. Mongin, R. Uribe, J. Puy, J. Cecilia, J. Galceran, H. Zhang, W. Davison, Key
752 Role of the Resin Layer Thickness in the Lability of Complexes Measured by DGT,
753 Environ. Sci. Technol., 45 (2011) 4869-4875.

754 67. R. Uribe, S. Mongin, J. Puy, J. Cecilia, J. Galceran, H. Zhang, W. Davison,
755 Contribution of Partially Labile Complexes to the DGT Metal Flux, Environ. Sci.
756 Technol., 45 (2011) 5317-5322.

757

758

Figures

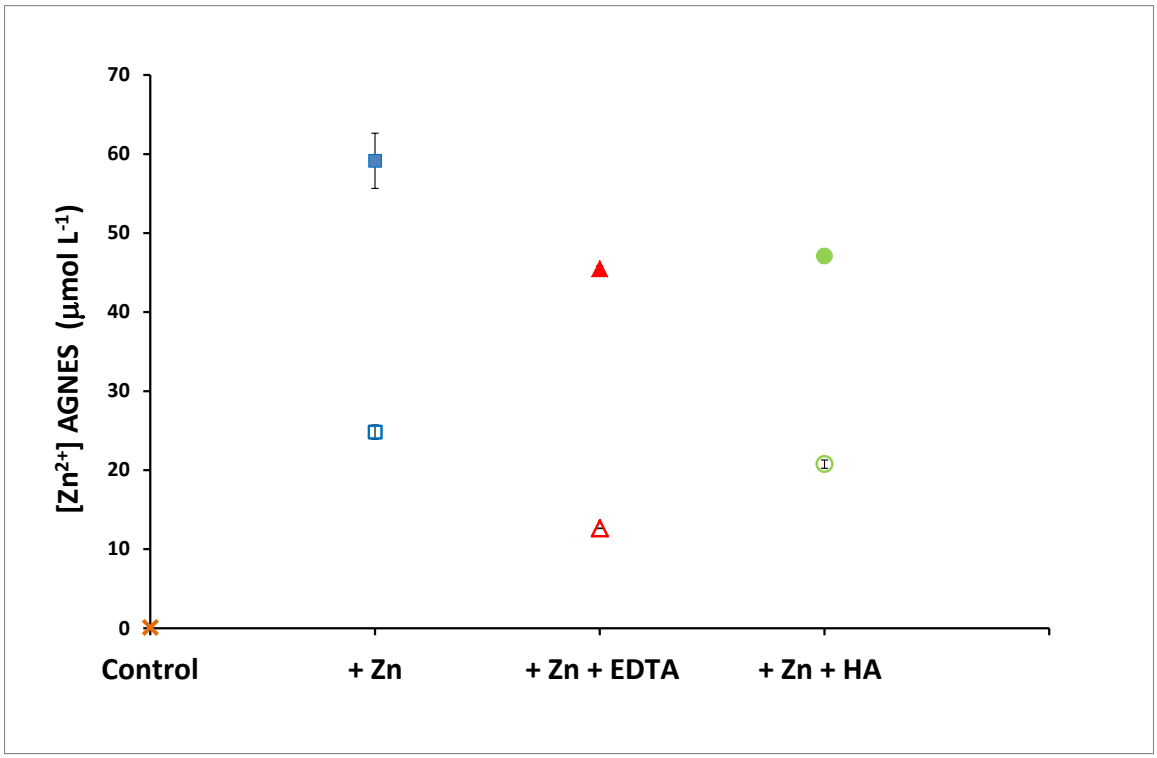

Figure fig_AGNES 1. Free $[Zn^{2+}]$ measured with AGNES in the different hydroponic media. Empty markers correspond to an added $c_{T,Zn}$ =3.50×10^{-5} mol L^{-1} and full markers to 6.96 10^{-5} mol L^{-1}. Orange cross: control medium (see Section 2.2); blue squares: control media with an added extra Zn concentration; red triangles: control media with added Zn and EDTA (20 µmol L^{-1}); green circles: control media with added Zn and humic acid (60 mg L^{-1}). Error bars represent the standard deviation (if larger than the markers) corresponding to replicates of two independent samples. (correlacions_Exces_v18.xls /G_AGNES)

774

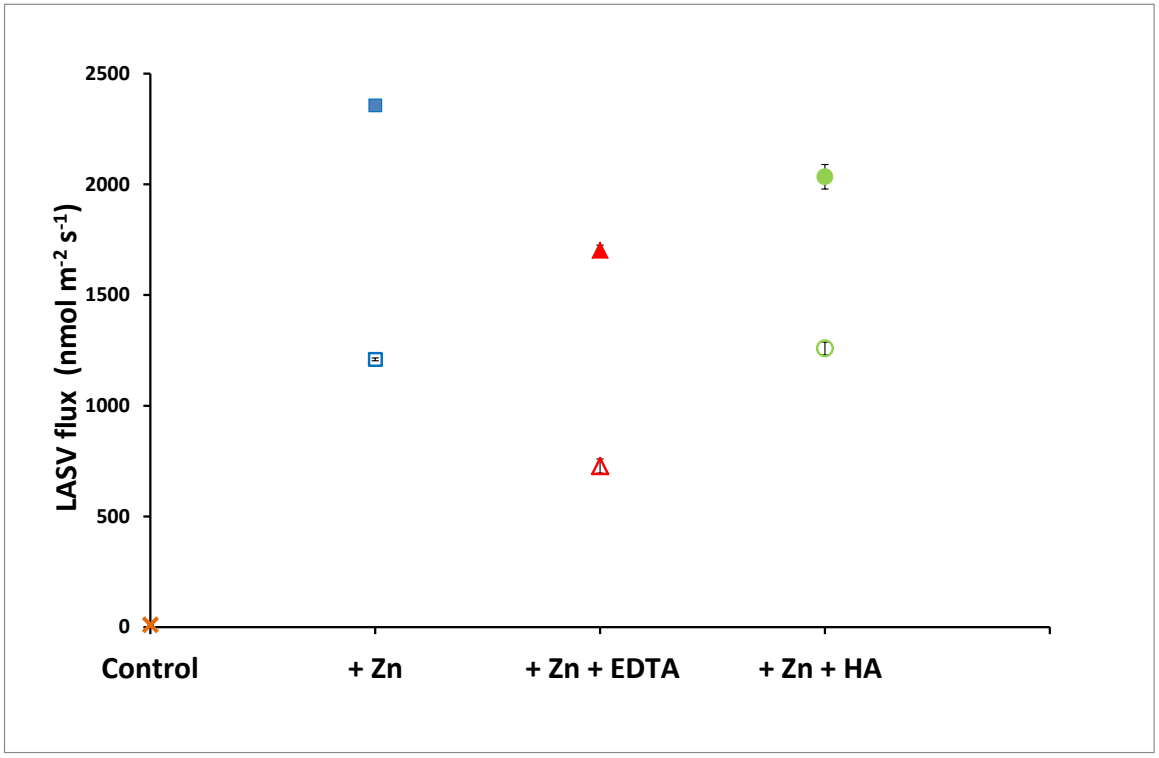

775

776 Figure Fig_ASV_systems2: Zn flux measured with LASV (with linear stripping) in the
777 different media. Markers as in Fig 1. Error bars represent the standard deviations (*n*=3),
778 whenever larger than the marker, corresponding to different determinations in the same
779 sample. (correlacions_Exces_v17.xls /G_SV)

780

781

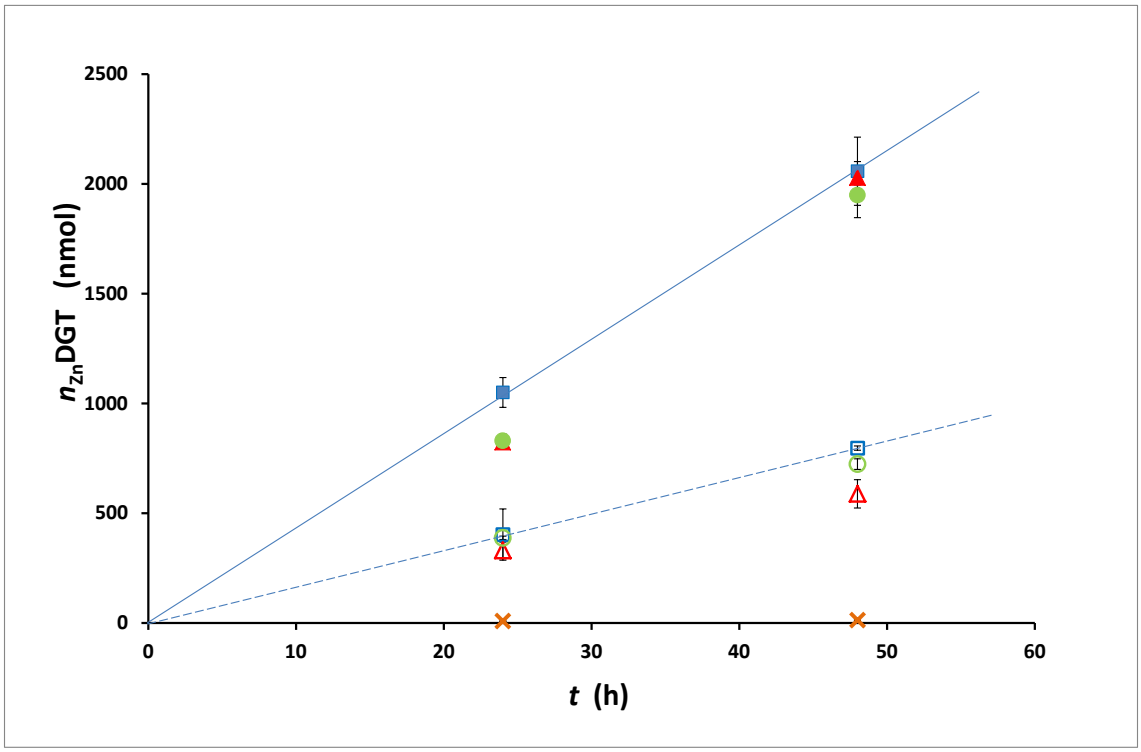

782

783

784 Figure fig_DGT3. Zn accumulated in DGT devices after 24 and 48 h. Markers as in Fig

785 fig_AGNES 1. Lines are an aid to the eye to show the linear regime for the case with just

786 added metal. Error bars represent the standard deviations (n=3), whenever larger than

787 the marker, corresponding to different determinations in the same sample.

788 (correlacions_Exces_v18.xls /G_DGT)

789

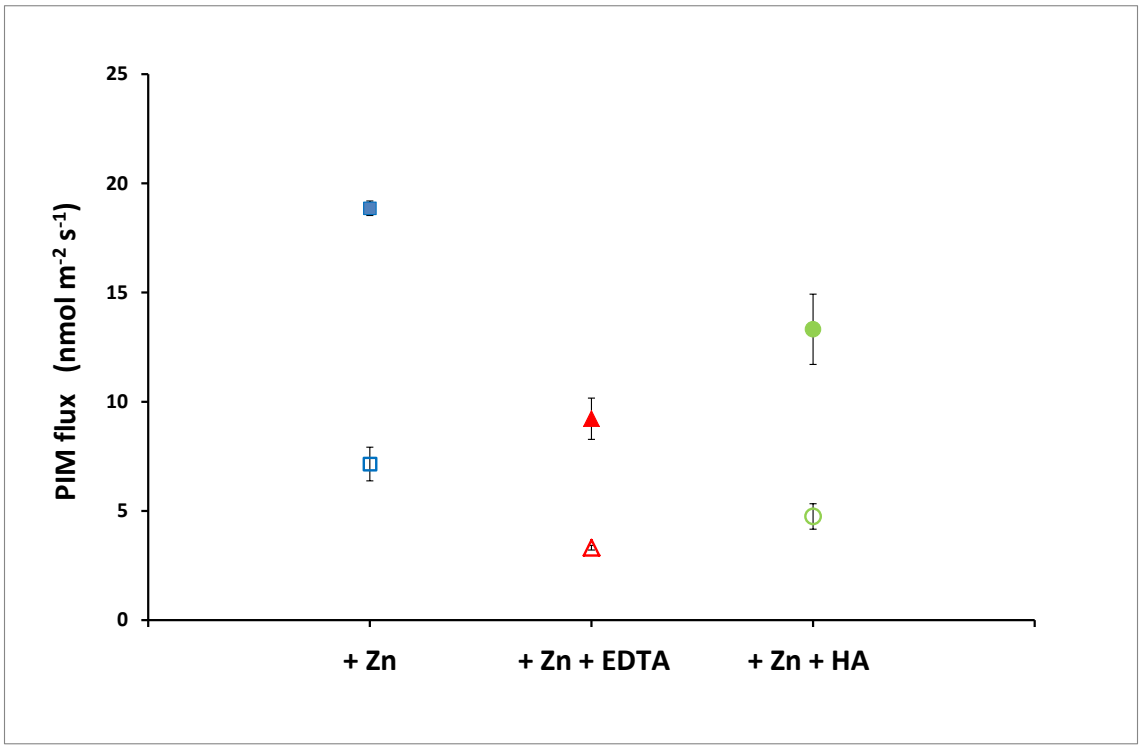

790

791 Figure fig_PIM_systems4. Zn flux measured with PIM-based devices in the different media.

792 Markers as in Fig fig_AGNES 1. Error bars represent the standard deviations (*n*=2 or 3)

793 corresponding to replicates of three independent samples. (correlacions_Exces_v18.xls

794 /G_PIM)

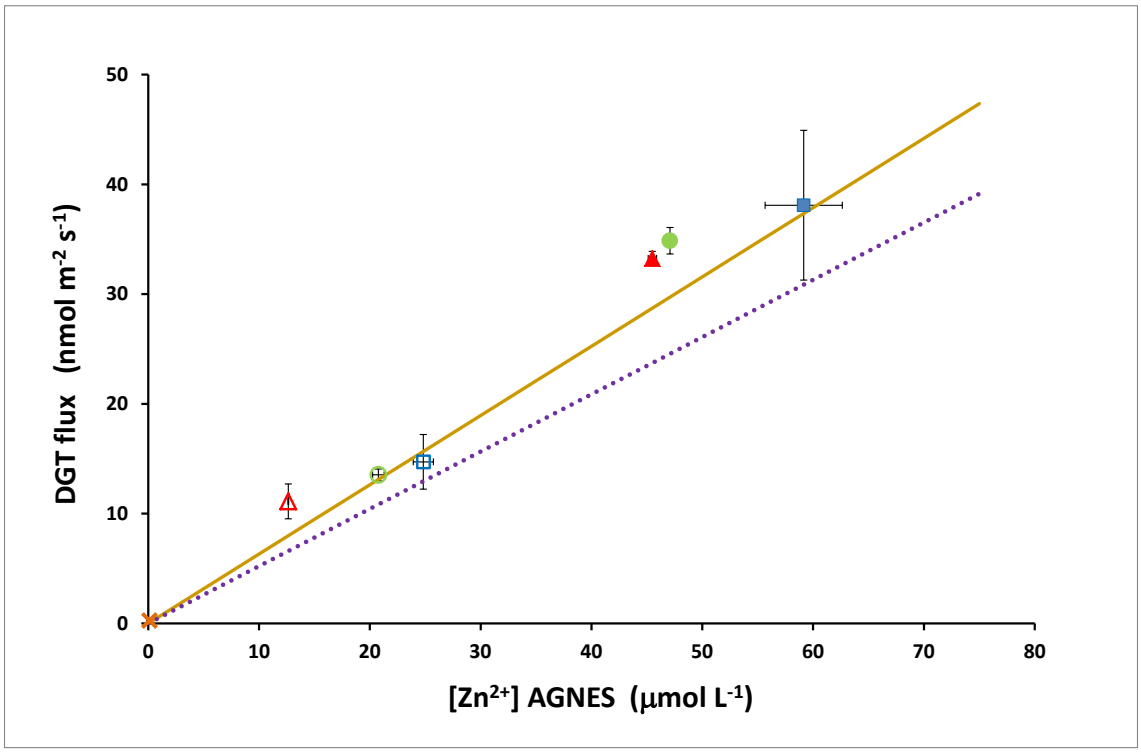

795

796 Figure fig_DGT_AGNES5. Zn flux with DGT versus free Zn concentration with AGNES.

797 Markers as in Fig fig_AGNES 1. Error bars as in previous figures. The brown continuous

798 line quantifies the contribution to the flux of free metal plus the complexes in the

799 Hoagland medium, i.e. $J_{\text{medium}} = \frac{D_{\text{M}}}{\delta}\left(1+K'\right)c_{\text{M}}$. The purple dotted line quantifies the free

800 metal contribution to the flux, i.e. $J_{\text{free}} = \frac{D_{\text{M}}}{\delta}c_{\text{M}}$ with D_{M}/δ obtained from equation

801 FactorFlux(10). (correlacions_Exces_v18.xls /G_DGT_AGNES)

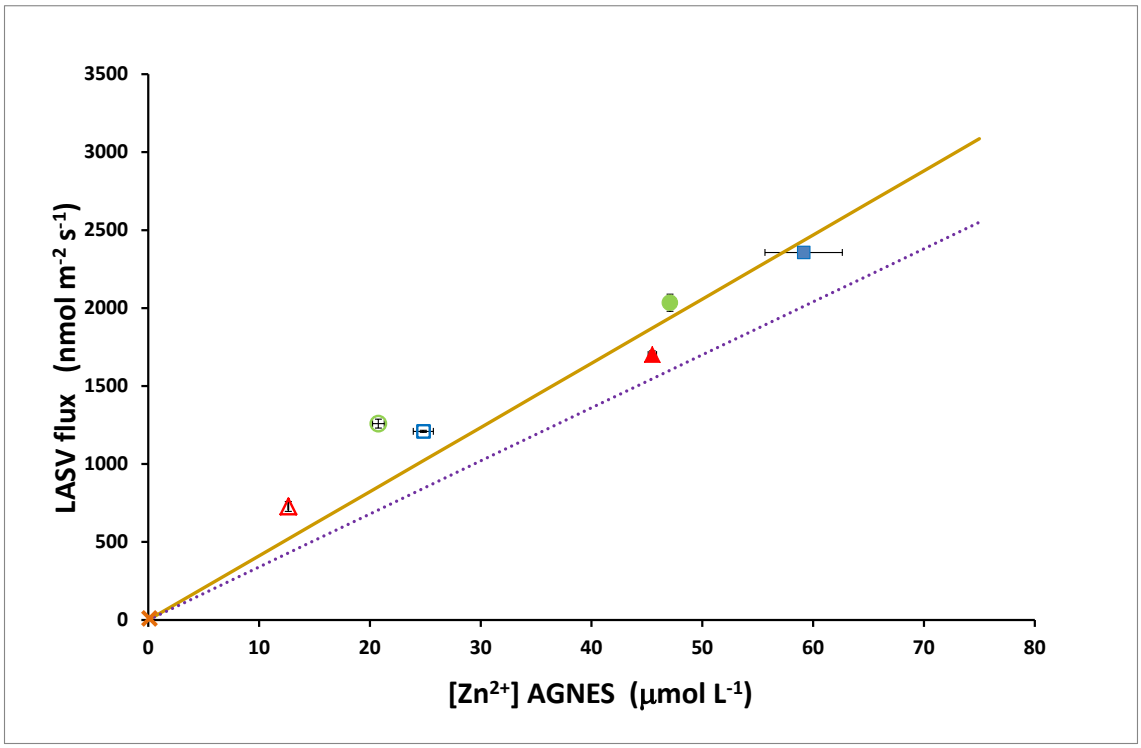

Figure fig_SV_AGNES6. Zn flux obtained with LASV versus free Zn concentration obtained with AGNES. Markers as in Fig fig_AGNES 1. Error bars as in previous figures. Lines as in previous figure(correlacions_Exces_v18.xls /G_SV_AGNES).

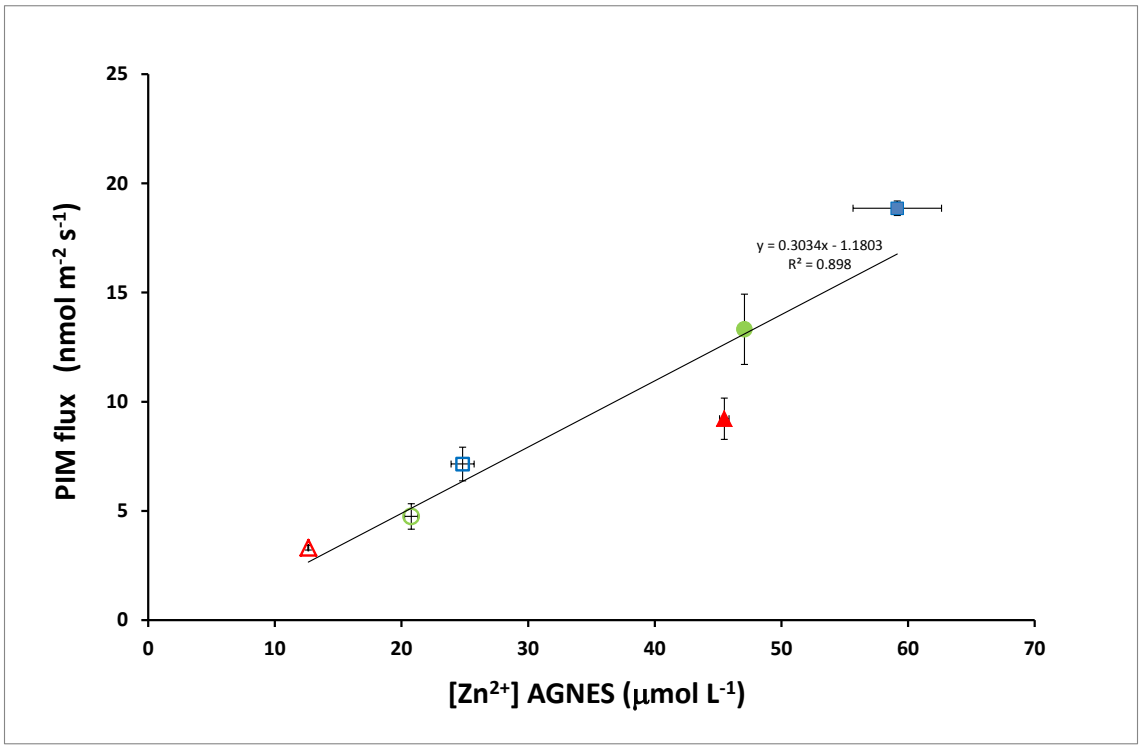

806

807 Figure fig_PIM_AGNES7. Zn flux measured with PIM versus free Zn concentration with
808 AGNES. Markers as in Fig fig_AGNES 1. Error bars as in previous figures . The added
809 straight line is the global regression of the plotted data (correlacions_Exces_v18.xls
810 /G_PIM_AGNES).

811
812

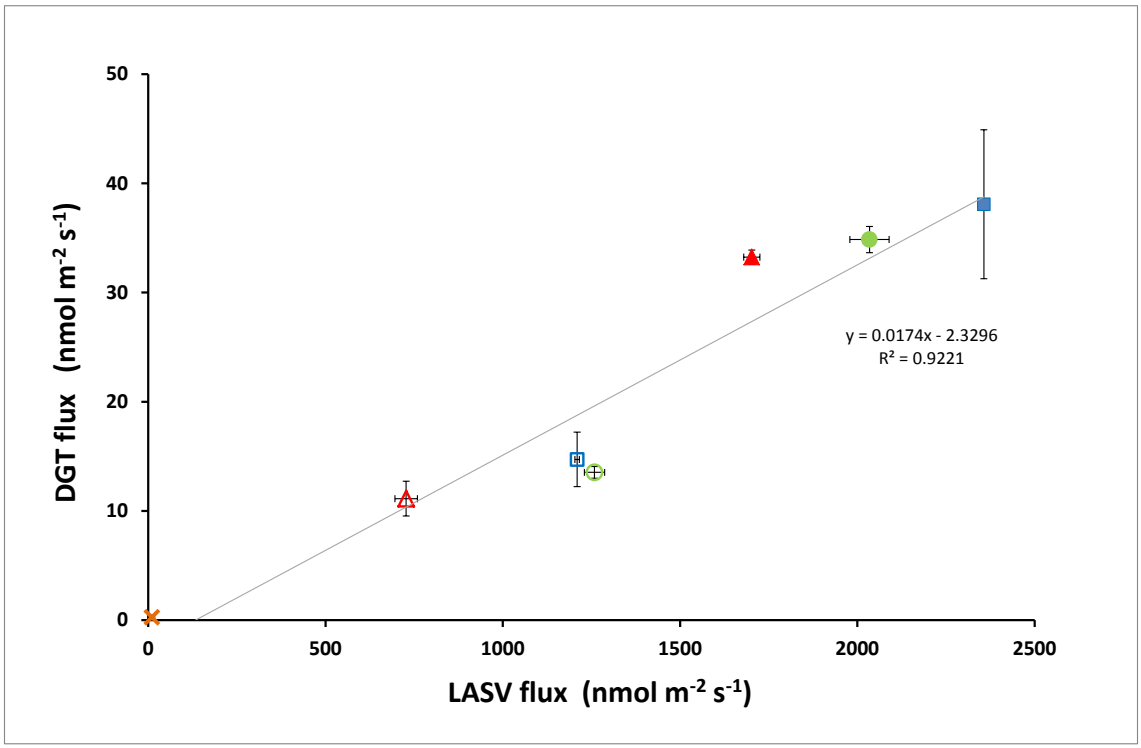

Figure fig_DGT_SV8. Zn flux with DGT versus Zn flux with LASV. Markers as in Fig fig_AGNES 1. Error bars as in previous figures. (correlacions_Exces_v18.xls /G_DGT_SV)) The added straight line is the global regression of the plotted data.